COMMUNICATION

ChemComm
www.rsc.org/chemcomm

Investigation of the morphology–catalytic reactivity relationship for Pt nanoparticles supported on alumina by using the reduction of NO with CH_4 as a model reaction

Ioan Balint,*[a] Akane Miyazaki[b] and Ken-ichi Aika[b]

[a] *Institute of Physical Chemistry, Romanian Academy, Spl. Independentei 202, 77208 Bucharest, Romania. E-mail: balint@chemenv.titech.ac.jp*

[b] *Department of Environmental Chemistry and Engineering, Interdisciplinary Graduate School of Science and Technology, Tokyo Institute of Technology, 4259 Nagatsuta, Midori-ku, 226-8502 Yokohama, Japan. E-mail: kenaika@chemenv.titech.ac.jp*

Received (in Cambridge, UK) 11th March 2002, Accepted 28th March 2002
First published as an Advance Article on the web 12th April 2002

The morphological evolution of large Pt nanoparticles supported on alumina in reaction conditions has a significant impact on the catalytic behaviour for the NO/CH_4 reaction.

Great efforts are currently being made to better understand the relationship existing between the structure of a supported metal and the related catalytic reactivity.[1] It is clear that significant improvements in the catalytic behaviour can be achieved through an adequate morphological control of the supported metal particles. Additionally, the reaction mechanism becomes more clear when well-defined metal particles are used as catalysts. A bridge between real catalysis and high vacuum studies, focusing mainly on the elementary reaction steps, can thus be foreseen.

Morphological control is difficult when classical methods [*i.e.* support impregnation with metal precursor(s), calcination, reduction, *etc.*] are used for catalyst preparation because the final characteristics of the material are extremely sensitive to the history of preparation. Additional complexity arises from the fact that the catalytic activity of the metals is considerably affected by the interaction with the support.[2]

One convenient way to minimize the preparation and support effects on the metal morphology, and thus on the catalytic reactivity, is the deposition of the well-defined metal nanoparticles on an oxide support. We have shown that, in spite of its acidity, alumina can be a suitable support for ammonia synthesis if uniform colloidal Ru nanoparticles of around 5 nm are supported on it.[3]

Large Pt nanocrystals of $\approx$13 nm supported on alumina exhibit significantly different catalytic behavior in a structure sensitive reaction (NO/CH_4) as compared with a conventional catalyst, having small Pt particles of around 1.8 nm.[4] The formation of NH_3 and CO is suppressed or greatly reduced whereas the production of N_2O is enhanced over the large, cubic Pt nanoparticles. Although it was suggested that both the size and facets might have a significant role in the catalytic behavior[5] some essential aspects still remain unclear. The morphological evolution of the Pt nanoparticles with time, in reaction conditions, as well as the effect of this evolution on the activity for the NO/CH_4 reaction have, until now, not been investigated. We show here, for the first time, that the morphological changes of the supported Pt nanoparticles, taking place in reaction conditions, have a considerable impact on the catalytic activity and selectivity for the NO/CH_4 reaction.

The preparation procedure of large, well-defined Pt nanocrystals has already been reported.[6] Briefly, the careful reduction of K_2PtCl_4 with H_2 at 40 °C in the presence of the polymer of NIPA (*N*-isopropylacrylamide) gives a large fraction of cubic Pt nanocrystals with an average size of $\approx$13 nm. Since the morphology of the Pt colloid changes slightly from batch to batch and the NO/CH_4 reaction is very sensitive on the metal structure it is our standard procedure to characterize the Pt colloid before deposition on alumina by TEM (Fig. 1a). Table 1 shows that around 70% of Pt nanoparticles in the colloidal stage (initial) had a square structure. The cubic nanoparticles relatively free of defects ($\approx$53%) are denoted as 'clear square' whereas the nanoparticles having defective, rough surfaces ($\approx$17%) are denoted as 'unclear square'. Besides the mainly cubic nanoparticles,

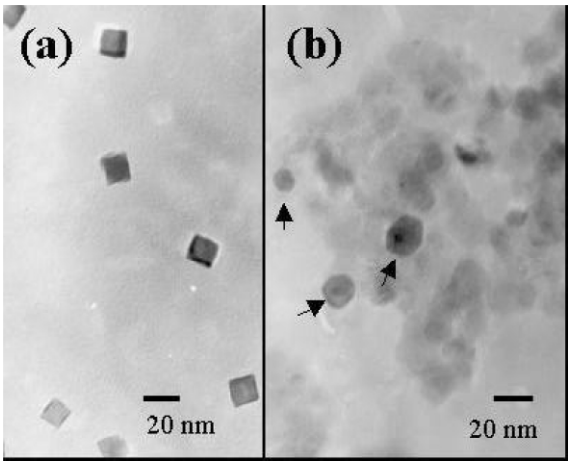

Fig. 1 TEM images of (a) Pt colloid composed mainly of square Pt nanoparticles ($\approx$70%), and (b) alumina supported Pt nanoparticles (irregular, hexagonal and round ones) aged in an NO/CH_4 mixture at 950 °C for 4 h (Pt particles are indicated by arrows).

Table 1 The morphology of Pt nanocystals in the initial and final state of the catalyst [Pt colloid, after Pt deposition on alumina, after catalyst aging at high temperature (950 °C, 4 h) in an NO/CH_4 reaction mixture] as determined by TEM and XRD

	Average size/nm		Morphological distribution[a] (%)					
Stage	d_{TEM}[a]	d_{XRD}[b]	Clear square	Unclear square	Hexagonal	Round	Small	Irregular
Initial[c]	13.3	11.7	53	17	9	5	5	11
Final[d]	16.3	10.6	0	6.4	17.2	25.5	3.6	47.3

[a] Morphological characterization (size and morphological distribution) was statistically determined by TEM by counting more than 300 particles. [b] Size was calculated from the broadening of XRD peak of Pt(111) ($2\theta \approx 40°$) after supporting platinum nanoparticles on alumina. [c] Morphology of the supported Pt nanocrystals prior to catalytic reaction. [d] Morphology of the catalyst aged at 950 °C for 4 h in an NO/CH_4 reaction mixture.

DOI: 10.1039/b202421g

shapes such as irregular, hexagonal and round as well as 'small' were also observed.

The supporting procedure of the colloidal Pt nanoparticles on alumina has already been described.[4,5] TEM and XRD observations confirmed that the morphology of the Pt nanoparticles did not change after supporting them on alumina. The size of the supported Pt crystallites was estimated from the broadening of the Pt(111) XRD peak at $2\theta \approx 40°$ by using the Debye–Scherer equation. As can be seen in Table 1, the d_{TEM} of 13.3 nm is in fairly good agreement with d_{XRD} of 11.7 nm. The determination of the metal surface area by CO or by H_2 chemisorption is not relevant because the exposed surface of the large Pt particles is very small. Theoretical calculations, by considering an average particle size of 13 nm, gives a platinum dispersion of around 6%, that is too small to be accurately measured.

The catalytic tests for the NO/CH_4 reaction were performed in the temperature range 350–600 °C by using a quartz reactor loaded with 0.05 g of catalyst (1% Pt/Al_2O_3). The gas hourly space velocity (GHSV) of the reactant mixture (0.41% CH_4, 1% NO and balance Ar) was 60000 h^{-1} (the total flow rate of the reactant mixture was 50 cm^3 min^{-1} STP).

The NO was practically completely converted to reaction products over the fresh catalyst starting from 350 °C. After the first test, the catalyst was subjected to an accelerated thermal aging at 950 °C for 4 h in the NO/CH_4 reaction mixture. This allowed us to observe the morphological changes taking place with the well-structured (manly cubic) Pt nanocrystals during aging as well as the effect of this evolution on the catalytic performances. The catalytic behaviour of the aged catalyst for the NO/CH_4 reaction was then checked again in the low temperature region (350–600 °C). The observed modifications can be summarized as follows: (i) the catalytic activity for NO conversion decreased slightly (the temperature for the total conversion of NO was shifted from 350 to 400 °C), (ii) the production of N_2O and CO decreased significantly and (iii) the formation of NH_3 was prevented.

Fig. 2 illustrates the aging effect on the catalytic behaviour of alumina supported Pt nanoparticles. For simplicity only the yields to the harmful products (N_2O, CO, and NH_3) are compared (the selectivity to N_2, CO_2 and H_2 is omitted). Aging depressed the formation of N_2O in the whole temperature domain investigated. Another positive benefit of the morphological evolution of the Pt nanoparticles is the complete suppression of NH_3 formation and the significant decrease in CO production. The yield to CO becomes negligible below 550 °C whereas for higher temperatures it decreases sharply compared to the fresh catalyst.

The data presented in Table 1 shows that: (i) the size of Pt nanocrystals seems to be not significantly altered by aging and (ii) the Pt nanocrystals are undergoing a significant facet restructuring during the high temperature treatment. The larger d_{TEM} (16.3 nm) as compared with d_{XRD} (10.6 nm) for the aged catalysts can be explained rather by the flattening of the Pt particles on the support than by sintering because no sign of particle agglomeration was observed. The initially 'clear square' Pt nanoparticles were completely converted to round ($\approx$25.5%), irregular ($\approx$47.3%) and hexagonal ($\approx$17.2%) shaped particles (see Table 1). A small amount ($\approx$6.4%) of 'unclear square' Pt particles could be still identified after the restructuring of the cubic Pt particles. In other words the low index facets were gradually shifted in high temperature reaction conditions to higher index planes.

From the clean surface chemistry, performed in high vacuum conditions, it is well known that the low index Pt planes, *i.e.* Pt(100),[7] are less active for NO dissociation as compared with the higher index planes, *i.e.* Pt(410).[8] The surface defect (steps, kinks) sites are also very efficient for NO decomposition.[9] On the low index Pt nanoparticles, having low concentrations of surface defects, only a fraction of the adsorbed NO dissociates in N_{ads} and O_{ads}. The yield of N_2O on the surfaces with low activity for NO decomposition is high because the reaction between NO_{ads} and N_{ads} is favored.[10] The high activity of the high index planes and of the surface defects for NO decomposition[8,9] explains well the decrease in the selectivity to N_2O, in parallel with the increase in N_2 yield *via* the reaction $N_{ads} + N_{ads} \rightarrow N_2$ (Fig. 2).

The small Pt particles strongly interact with the oxygen in reaction conditions forming PtO_x species (bulk oxide) with low oxidation activity.[11] On the other hand, the surface of the Pt nanoparticles will be covered only with a layer of reactive oxygen[12] because the properties of the large metal particles ($d >$ 5 nm) resembles those of the bulk metal.[13] The CH_x species formed by the dissociative adsorption of CH_4 will be further oxidized to CO_x by oxygen resulting from the dissociation of NO. The low activity of well-structured (cubic) Pt nanocrystals for NO decomposition reduces the supply of active oxygen for CH_x oxidation and therefore the catalyst will exhibit a higher yield to CO as compared with the restructured Pt nanoparticles (Fig. 2). The high activity of the restructured Pt nanoparticles for NO decomposition increases the supply of active oxygen which rapidly removes the surface carbonaceous species as CO_2. The above-proposed mechanism is sustained also by the fact that the reaction selectivity to hydrogen (not presented here) decreased for the restructured Pt particles.

It is accepted that NH_3 is formed in the reactions between N_{ads} (resulted from NO decomposition) and a hydrogen source which can be either CH_x or H_{ads} (both resulting from CH_4 splitting).[14] The larger amount of oxygen available on the surface of the restructured Pt favours the removal, as oxidation products (CO_2 and H_2O), of the hydrogen sources (CH_x and H_{ads}) responsible for ammonia formation. Therefore the reaction between N_{ads} and N_{ads} becomes a favoured one in comparison with the reaction of ammonia formation (*i.e.* $N_{ads} + [H]_{source} \rightarrow NH_3$).

A research fund from the Japanese Society for the Promotion of Science (No. P00136) is greatly appreciated.

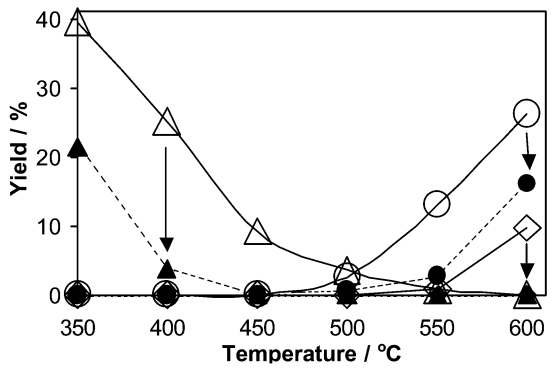

Fig. 2 Comparison between the NO/CH_4 reaction yield to N_2O (△, ▲), CO (○, ●) and NH_3 (◇, ◆) for the fresh (open symbols) and aged (closed symbols) alumina-supported Pt nanoparticles in the 350–600 °C temperature range (reactant mixture: 0.41% CH_4, 1% NO and balance Ar).

Notes and references

1 B. C. Gates, *Chem. Rev*., 1995, **95**, 511.
2 J. M. Rickard, L. Genovese. A. Moata and S. Nitsche, *J. Catal*., 1990, **121**, 141.
3 A. Miyazaki, I. Balint and K-i. Aika, *J. Catal*., 2001, **204**, 364.
4 I. Balint, A. Miyazaki and K-i. Aika, *Chem. Lett*., 2001, 1024.
5 I. Balint, A. Miyazaki and K-i. Aika, *Appl. Catal. B*, 2002, **37**, 217.
6 A. Miyazaki and Y. Nakano, *Langmuir*, 2000, **16**, 7109.
7 C. M. Comrie, W. H. Weinberg and R. M. Lambert, *Surf. Sci*., 1976, **57**, 619.
8 W. F. Banholzer and R. I Masel, *J. Catal*., 1984, **85**, 127.
9 T. Zambelli, J. Wintterlin, J. Trost and G. Ertl, *Science*, 1996, **273**, 1688.
10 T. W. Root and L. D. Schmidt, *Surf. Sci*., 1983, **134**, 30.
11 R. F. Hicks, H. Qi, M. L. Young and R. G. Lee, *J. Catal*., 1990, **122**, 280.
12 E. S. Putna, J. M. Vohs and R. J. Gorte, *Surf. Sci*., 1997, **391**, L1178.
13 M. Boudart, *J. Mol. Catal*., 1985, **30**, 27.
14 R. Burch and A. Ramli, *Appl. Catal. B*, 1998, **15**, 63.